A Mechanistic Framework for the Second Step of Splicing Catalyzed by the *Tetrahymena* Ribozyme†

Philip C. Bevilacqua,‡ Naoki Sugimoto,§ and Douglas H. Turner*

Department of Chemistry, University of Rochester, Rochester, New York 14627-0216

Received August 18, 1995; Revised Manuscript Received November 9, 1995⊗

ABSTRACT: A simple model system is described which mimics the second step of splicing and reverse cyclization reactions of the self-splicing intron from *Tetrahymena thermophila.* This model is based on the L-21 Sca I catalyzed ligation reaction between exogenously added oligomers: cucu + UCGa $\overset{\text{L-21 Sca I}}{\rightleftharpoons}$ cucua + UCG. Steady-state kinetics for the forward and reverse direction were measured at 15 °C to find oligonucleotides that exhibit Michaelis−Menten behavior with acceptable K_Ms. CUCU and UCGA fit both criteria and were chosen for further studies. Steady-state kinetics reveal a lag that appears to be an RNA folding step that is eliminated by preincubation of the ribozyme with 2 mM and higher [Mg^{2+}] and by UCGA. At constant ionic strength, the Mg^{2+} dependence of steady-state rates exhibits a sharp maximum near 5 mM Mg^{2+}. Pre-steady-state and steady-state kinetics, along with active-site titrations, explain the Mg^{2+} profile: the rate of reaction up to and including chemistry increases with Mg^{2+} concentration, while the fraction of active ribozyme and the rate of postchemistry steps decrease with Mg^{2+} concentration. The rate-limiting step at 5 mM Mg^{2+} for the reaction mimicking the second step of splicing is either chemistry or a conformational change before chemistry involving ribozyme bound with substrates. The rate-limiting step at 50 mM Mg^{2+} appears to be a postchemistry conformational change of the ribozyme or product release. At 50 mM Mg^{2+}, single-turnover experiments support ordered binding of substrates with 5′-exon mimic binding before 3′-splice site mimic. Moreover, the 3′-splice site mimic binds and reacts in the presence of 5′-exon mimics *predocked* into the catalytic core. Results also indicate that Mg^{2+} ions associate with the ribozyme upon docking.

The mechanism of group I ribozyme-catalyzed reactions has been the subject of intense investigation. Most studies have focused on reactions that model the first step of splicing, i.e., G-addition (Cech et al., 1992, and references therein; Herschlag et al., 1993a,b; McConnell et al., 1993; Piccirilli et al., 1993; Bevilacqua et al., 1994; Herschlag & Khosla, 1994; McConnell & Cech, 1995; Narlikar et al., 1995). The purpose of the work presented here is to develop a framework for studying the second step of splicing. While the first and second steps of splicing are the chemical reverse of each other (Figure 1), differences between them exist. One difference is that, in the second step of splicing, the 3′-splice site is at the G binding site and employs additional base-pairing between the core of the ribozyme and the two nucleotides immediately upstream of the 3′-splice site in a pairing termed P9.0 (Figure 1). This pairing positions the 3′-splice site next to P7 and the G-binding site (Burke, 1989; Michel et al., 1989, 1990; Burke et al., 1990).

In this paper, the L-21 Sca I truncated form of the group I self-splicing intron from *Tetrahymena thermophila* (Inoue & Kay, 1987, Zaug et al., 1988) is used to develop a model system for the second step of splicing, i.e., exon ligation, and for the reverse-cyclization reaction (Figure 1) (Sullivan & Cech, 1985; Sugimoto et al., 1988). We began to mimic the second step of splicing with the minimal model developed using CU and GA in the presence of L-21 Sca I (Inoue & Kay, 1987). We find, however, that CUCU is the minimal-length 5′-exon mimic with simple Michaelis−Menten kinetics behavior, and UCGA is the optimal 3′-splice site mimic since it has tight binding (Tanner & Cech, 1987; Price & Cech, 1988; Moran et al., 1993) and allows the P9.0 pairing to form. It is worth noting that while the summary scheme in Figure 1 is correct in showing CUCUA for the 5′-splice site mimic, the wild-type 3′-splice site is UCGU, not UCGA. However, in model reactions between CU and GN (where N is A, C, or U) using L-21 Sca I, little difference in rate was observed for the different GN substrates, suggesting the identity of the N position is not critical (Inoue & Kay, 1987). In addition, Narlikar et al. (1995) present evidence that the identity of the A in CCCUCUA is not important to transition state destabilization. Also, UCGA represents the correct reaction site for reverse-cyclization (Sullivan & Cech, 1985; Sugimoto et al., 1988).

Steady-state and pre-steady-state kinetics are used to study this model system. Steady-state kinetics are used to identify substrates that follow typical hyperbolic Michaelis−Menten kinetics, to explore salt conditions, and to establish a renaturation protocol for the ribozyme. Pre-steady-state kinetics are used to provide rates for individual steps and to examine the position of rate-limiting steps for both the forward and reverse directions of the overall mechanism at Mg^{2+} concentrations of 5 and 50 mM. The results identify potential conformational changes, reveal the Mg^{2+} dependence of the reaction, and provide a framework for more detailed experiments.

† This work was supported by NIH Grant GM22939.

* Author to whom correspondence should be addressed.

‡ Current address: Department of Chemistry and Biochemistry and the Howard Hughes Medical Institute at the University of Colorado, Boulder, CO 80309-0215.

§ Current address: Department of Chemistry, Faculty of Science, Konan University, 8-9-1 Okamoto, Higashimada-ku, Kobe 658, Japan.

⊗ Abstract published in *Advance ACS Abstracts,* December 15, 1995.

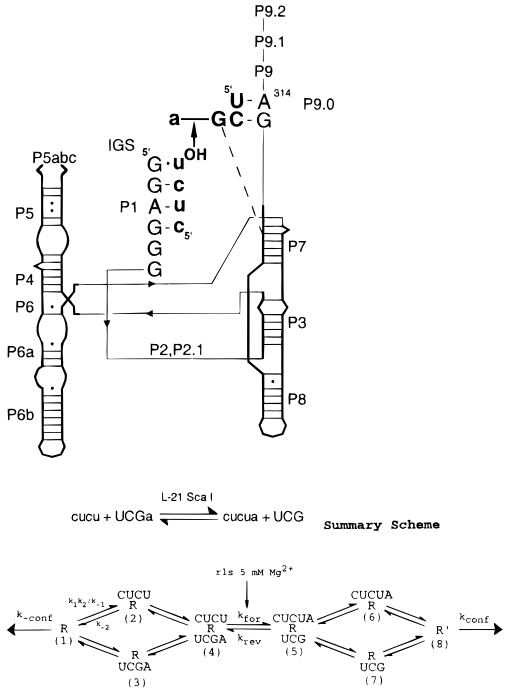

FIGURE 1: Secondary structure of the catalytic core of the group I intron from *T. thermophila* (Cech et al., 1994). Peripheral helices (P2, P2.1, P5a−c, P9, P9.1, and P9.2) present in L-21 Sca I are listed but not drawn. Oligonucleotide cucu is bound to the internal guide sequence (IGS) GGAGGG to form the P1 pairing, and UCGa is bound to the G-binding site, indicated with a dashed line, and forms the P9.0 pairing with $G^{313}A^{314}$ of the ribozyme. Intron-mimic sequences are in uppercase letters and exon-mimic sequences in lowercase letters. Watson−Crick base pairs are indicated with dashes and GU pairs with dots. The 5′-ends of L-21 Sca I, cucu, and UCGa are indicated. The summary scheme shows the L-21 Sca I catalyzed ligation reaction between cucu and UCGa. The forward direction mimics both the second step in splicing, i.e., exon ligation, and also reverse cyclization. The reverse direction mimics the first step in splicing, i.e., G-addition, and also intron cyclization. The overall scheme shows the rate-limiting step (rls) at 5 mM Mg^{2+} for the forward reaction, and each species is numbered for identification. R is the ribozyme, L-21 Sca I. k_{for} is a rate constant due to combination of all unimolecular steps (with rates k_i) requiring both substrates up to and including chemistry for the forward reaction; $k_{for}^{-1} = \sum_i k_i^{-1}$, where one of the k_i must be k_{chem}, the rate of the forward chemical step (Fersht, 1985). The rate k_{rev} is analogous to k_{for}, but for the reverse reaction. The rate constants k_{conf} and k_{-conf} are rate constants for conformational changes for the forward and reverse reactions, respectively.

MATERIALS AND METHODS

Materials. CU, GA, and pdG were obtained from Sigma, and their purity was confirmed by normal phase TLC (Baker Si250F plates with the solvent *n*-propanol/NH_4OH/H_2O, 55:35:10) and reversed-phase HPLC (Longfellow et al., 1990). Trimer and longer oligonucleotides were synthesized on solid support by a phosphoramidite method (Kierzek et al., 1986) and purified by HPLC (Longfellow et al., 1990).

Concentrations of oligomers were determined optically at 260 nm (Borer, 1975; Richards, 1975). Oligomers were 5′-end-labeled and purified as previously described (Bevilacqua & Turner, 1991). L-21 Sca I ribozyme (Zaug et al., 1988) was prepared as previously described (Bevilacqua & Turner, 1991). Except where noted, L-21 Sca I was renatured and preincubated as described (Bevilacqua & Turner, 1991) followed by a 10−16 h preincubation at 15 °C in reaction buffer.

Kinetics. All kinetics experiments were run with the L-21 Sca I ribozyme in reaction buffer of 50 mM Hepes (25 mM M^+), pH 7.4, at 15 °C and varying amounts of NaCl and $MgCl_2$. For the Na^+ Hepes buffer, an equal amount of the Na^+ and H^+ salts of Hepes were used. (The pK_A of Hepes is 7.5.) Unless otherwise noted, reactions were initiated by mixing a 2× solution of L-21 Sca I in reaction buffer with an equal volume of 2× solution of both substrates in reaction buffer. Steady-state kinetics were performed with the concentrations of substrates at least 20-fold greater than [L-21 Sca I]. All reactions were quenched as previously described (Bevilacqua & Turner, 1991). Products and reactants were separated by electrophoresis on 20% acrylamide/8 M urea gels. Bands were visualized by autoradiography, cut out, and quantified by scintillation counting. Kinetic plots were fit by a nonlinear least-squares method. Initial rate determinations were limited to the linear portion of the reaction, usually no more than 30% conversion of the limiting substrate. General conditions of concentration and mixing for each kinetic method are described in Results, and specific conditions are listed in the appropriate table.

RESULTS

Presentation and discussion of results is facilitated by reference to the overall scheme in Figure 1. This scheme presents the minimal framework required to account for the kinetic results at both 5 and 50 mM Mg^{2+}. A rate constant for substrate S in the absence of another substrate will be denoted k(S) and in the presence of another substrate k'(S).

At least one of the steps is more complex than illustrated. Binding of CUCU to L-21 Sca I (species 1 to 2) involves at least two steps: base-pairing at forward and reverse rates k_1 and k_{-1}, followed by formation of tertiary contacts at forward and reverse rates k_2 and k_{-2} (Bevilacqua et al., 1992; Herschlag, 1992). For CUCU and shorter 5′-exon mimics at 15 °C, the two-step process can be represented by the one-step process illustrated in the overall scheme in Figure 1 with $k_{on} = k_1k_2/k_{-1}$ and $k_{off} = k_{-2}$ (Bevilacqua et al., 1992).

The overall scheme in Figure 1 shows random sequential binding of both substrates and both products. Evidence for this will be presented: (1) p*CUCUA reacts in pulse−chase experiments at 50 mM Mg^{2+}, indicating that it can bind to free ribozyme and that UCG can bind to the p*CUCUA·R complex formed to obtain species 5, which then reacts. Herschlag and Cech (1990) present evidence for random binding of G and 5′-splice site mimics at 50 °C, suggesting UCG should also be able to bind independently. (2) CUCU traps in pulse−chase experiments at 50 mM Mg^{2+}, indicating it can bind to free ribozyme and that UCGA can bind to the p*CUCU·R complex to obtain species 4. (3) The fact that UCGA undergoes hydrolysis in the absence of CUCU indicates it can bind alone to ribozyme to give species 3. There is no direct evidence for the pathway between species 3 and 4 since UCGA does not react in pulse−chase experiments (although absence of reaction in pulse−chase experiments does not preclude this pathway). Evidence will be presented that this pathway is unfavored at 50 mM Mg^{2+}.

Steady-State Kinetics

The steady-state scheme for CUCU is shown in Figure 2. Similar schemes can be derived for 3′-splice site mimics. At 5 mM Mg^{2+}, p*CUCUA does not react in a pulse−chase

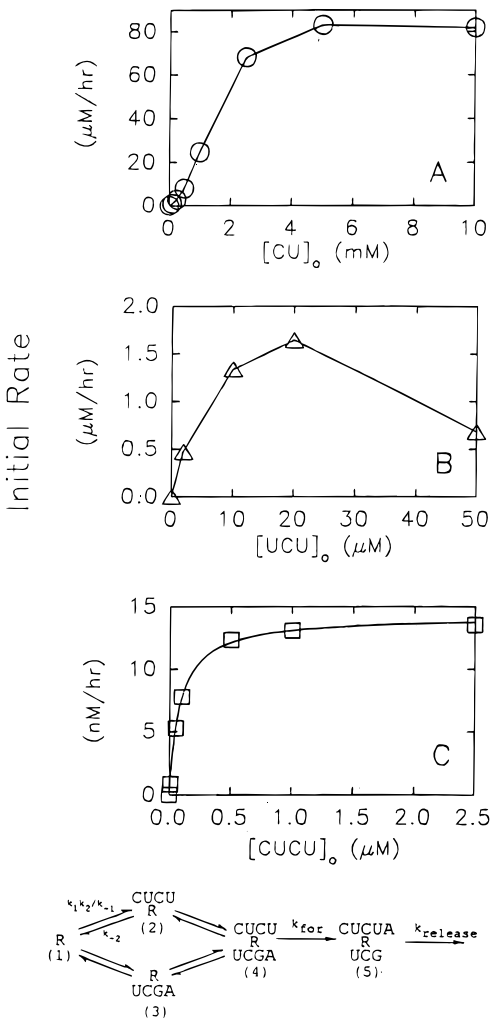

FIGURE 2: CUCU is the shortest 5′-exon mimic that exhibits well-behaved kinetics. Buffer for A−C is 50 mM Hepes (25 mM Na^+), pH 7.4, and 50 mM $MgCl_2$, with no NaCl added. In these experiments the ribozyme was not renatured or preincubated. Under the conditions of high [Mg^{2+}] and [GA] used here, no lag was observed. Similar experiments with renatured and preincubated ribozyme give similar results. All plots are of initial rate, using 5 mM GA for the 3′-splice site mimic. (A) Plot for CU in 5 μM L-21 Sca I (○). When corrected for the fraction of ribozyme unable to bind substrate (Bevilacqua & Turner, 1991), the limit at saturation gives an apparent k_{cat} for CU of $80/(5 \times 60 \times 0.3) = 0.9$ min^{-1}. (B) Plot for UCU in 0.1 μM L-21 Sca I(△). (C) Plot for CUCU in 1 nM L-21 Sca I (□). k_{cat} (corrected for ribozyme unable to bind substrate) and K_M for CUCU are 0.80 min^{-1} and 0.084 μM, respectively. The steady-state scheme is shown for CUCU and UCGA. $k_{release}$ includes all CUCUA and UCG release steps and any conformational changes of the ribozyme at rate k_{conf}.

experiment (see pre-steady-state results below), indicating its dissociation is rapid relative to k_{rev}, the rate constant for going form species 5 to 4; thus, k_{rev} at 5 mM Mg^{2+} can be ignored and k_{for} considered irreversible. (Only the radiolabeled substrate, in this case p*CUCUA, has to dissociate to preclude an observable reverse reaction.) At 50 mM Mg^{2+}, there is a burst for the forward reaction, indicating that k_{for} and at least one of the product release steps are rapid relative to a subsequent slow step (see pre-steady-state results); thus, k_{for} can also be considered irreversible at 50 mM Mg^{2+}. Moreover, under initial rate conditions, concentrations of the products, UCG and CUCUA, are low relative to the substrates, UCGA and CUCU, making all product release steps essentially irreversible.

Steady-state kinetics were fit to eq 1 (Fersht, 1985)

$$v_0 = \frac{k_{cat}[R]_o[S]_o}{K_M + [S]_o} \quad (1)$$

where v_o is the initial velocity of the reaction, $[R]_o$ is the initial concentration of ribozyme, $[S]_o$ is the initial concentration of the varied substrate, k_{cat} is the turnover number (eq 2), and K_M is the Michaelis constant (eq 3).

$$1/k_{cat} = 1/k_{for} + 1/k_{release} \quad (2)$$

$$K_M = \left(\frac{k_{for} + k_{off}}{k_{on}}\right)\left(\frac{k_{release}}{k_{release} + k_{for}}\right) \quad (3)$$

Here k_{on} and k_{off} are the rate constants for going between species 1 and 2. Equation 1 describes a simple hyperbola. Because K_M is the $[S]_o$ needed to obtain 1/2 V_{max} (where $V_{max} = k_{cat}[R]_o$ is the maximum initial velocity), it does *not* directly depend on $[R]_o$. k_{cat}, however, is obtained from the V_{max} asymptote and thus its calculated value depends on $[R]_o$. Values of k_{cat} at 50 mM Mg^{2+} in the text and tables are corrected for the 70% L-21 Sca I folded in a conformation that does not bind 5′-exon (Bevilacqua & Turner, 1991); figures, however, are uncorrected in order to visualize the effect of Mg^{2+} on the kinetics.

Both Mg^{2+} and the 3′-Splice Site Mimic Promote Ribozyme Folding. For multiple turnover reactions between UCGA and 2.5 μM CUCU, a lag is observed when L-21 Sca I is diluted into buffer immediately after thawing from −20 °C. In 5 mM Mg^{2+} with 1−25 μM UCGA, the lag time is longer the lower the [UCGA], lasting up to 7 h with 1 μM UCGA. In 5 mM Mg^{2+} with 25−200 μM UCGA, the lag time is constant at about 1.5 h. In 50 mM Mg^{2+} with 0.25−5 μM UCGA, the lag is between 1 and 2 h. In 50 mM Mg^{2+} with 5.0−50 μM UCGA, there is no observable lag. Apparently folding of an active ribozyme is assisted by high concentrations of Mg^{2+} and UCGA.

Kinetic plots after the lag time are linear for at least 24 h, suggesting any folding is completed during the lag (Bevilacqua, 1993). To test this, L-21 Sca I was preincubated in 2 mM Mg^{2+} for 10 h without any substrate, with 50 μM UCGA only, or with 2.5 μM CUCU only. Reaction was then initiated by addition of 2.5 μM CUCU, 50 μM UCGA, or both, as appropriate. In all these cases, the lag is eliminated and kinetic plots are linear from 0 to 10 h. This observation suggests the lag represents a rate-limiting conformational change that folds L-21 Sca I into a catalytically active form. To allow this folding step, in most of the experiments described below L-21 Sca I was renatured as described (Bevilacqua & Turner, 1991) and then preincubated in reaction buffer for 10−16 h before initiation of reaction. Similar observations and conclusions have been reported for related reactions under other conditions (Herschlag & Cech, 1990; Celander & Cech, 1991).

Optimal 5′ Exon Mimic for a Model of the Second Step of Splicing. A model system for the second step of splicing should have substrates with simple Michaelis−Menten kinetics. Another useful feature is minimal length of substrates so that off-rates for binding are structurally interesting, such as undocking for CUCU (Bevilacqua et al., 1992, 1993). Figure 2 shows plots of initial rate versus concentration for CU, UCU, and CUCU reacting with 5 mM

Table 1: Kinetic Parameters for CUCU and L-21 Sca I at 15 °C, pH 7.4, 50 mM Hepes/25 mM Na^+

3′ splice site mimic (mM)	[Mg^{2+}] (mM)[a]	[ribozyme] (mM)	[CUCU] (μM)	K_M (mM) steady state	k_{cat} (min^{-1})[b] steady state	k_{cat} (min^{-1})[b] burst	k_{cat}/K_M (M^{-1} s^{-1}) steady state	k_{for} (min^{-1}) pulse−chase	k_{for} (min^{-1}) single turnover	k_{for} (min^{-1}) burst[c]	k_{-2}' (min^{-1}) pulse−chase
multiple turnover											
GA 5[d]	50	0.001	varied	0.084	0.80		1.6×10^5				
UCGA 0.2	5	0.005	varied	0.9	0.72		1.3×10^4				
UCGA 0.5	5	0.002	varied	0.11	0.58		8.8×10^4				
UCGA 0.2	50	0.005	varied	1.8	0.21		2.0×10^3				
UCGA 0.5	50	0.002	varied	0.13	0.87		3.4×10^4				
burst											
UCGA 0.2	10	0.25	1.25			0.30				2.2	
UCGA 0.2	50	0.5 (0.25)	2.5 (1.25)			0.18				>1.5	
pulse−chase[e]											
UCGA 0.2	10	2.5	25					1.7−2.8			≤1
UCGA 0.2	50	2.5-10	25					1.8−2.8			≤1
single turnover											
UCGA 0.2	50	2.5	trace						1.1[f]		
									0.16[f]		

[a] Total ionic strength maintained at 175 mM with NaCl. [b] Data have been divided by the fraction of L-21 Sca I active under the specific salt condition (Bevilacqua & Turner, 1991) to obtain the listed *corrected* k_{cat}: at 5 mM Mg^{2+}, data are not corrected since all the ribozyme is active; at 50 mM Mg^{2+}, k_{cat} is divided by 0.3. Burst kcat data is from >1 turnover. [c] Burst k_{for} data is from <1 turnover. [d] This experiment was with ribozyme thawed directly from −20 °C into buffer. All other results are for renatured and preincubated ribozyme as described in text. [e] For pulse−chase experiments, [3′-splice site mimic] and [CUCU] are in chase and [ribozyme] is in the pulse. [f] Value of 1.1 is for 10 min preincubation of L-21 Sca I with CUCU. Value of 0.16 is for 10 min preincubation of L-21 Sca I with UCGA and a fit to a single-exponential equation, ignoring the lag.

GA in 50 mM Mg^{2+}. The initial rate plot for CU is sigmoidal at both subsaturating, 0.1 mM (data not shown), and saturating, 5 mM, concentrations of GA (Figure 2A). These plots are characteristic of cooperative behavior and suggest that, independent of GA saturation, binding of more than one CU may be required for reaction. Thus, CU is not an appropriate substrate for simple steady-state kinetic studies.

As shown in Figure 2B, steady-state kinetics for UCU show substrate inhibition. The initial rate plot for UCU in 5 mM GA is concave down with substrate inhibition at [UCU] > 20 μM. In addition, concentrations of UCGA above 25 μM inhibit UCU steady-state kinetics. Thus, UCU is not an appropriate substrate for simple steady-state kinetic studies because it gives substrate inhibition in a region before saturation and because it is unreactive in the presence of saturating amounts of the 3′-splice site mimic with the lowest K_M, UCGA.

Steady-state kinetics were measured for CUCU reacting with GA and UCGA. Below 50 μM CUCU, the initial rate plot for CUCU reacting with 5 mM GA in 50 mM Mg^{2+} has a hyperbolic shape, consistent with Michaelis−Menten kinetics (Figure 2C). K_M and k_{cat} are 84 nM and 0.80 min^{-1}, respectively (Table 1). Above 50 μM CUCU, substrate inhibition is observed; this concentration is far in excess of the [CUCU] required to saturate the binding site, however, and can thus be avoided. Hyperbolic behavior is also observed at 5 and 50 mM Mg^{2+} with 200 or 500 μM UCGA. CUCU appears to be the shortest 5′-exon mimic with relatively straightforward steady-state kinetics.

Rate Saturation Requires less CUCU at 500 μM UCGA Than at 200 μM UCGA. At 50 mM Mg^{2+}, K_Ms for CUCU are 1.8 and 0.13 μM in the presence of 200 and 500 μM UCGA, respectively. At 5 mM Mg^{2+}, K_Ms for CUCU are 0.9 and 0.11 μM in the presence of 200 and 500 μM UCGA, respectively. The changes in K_M for CUCU with UCGA concentration are summarized in the multiple-turnover section of Table 1. They could be at least partially due to a switch in the pathway for CUCU binding from species 1 to 2, to species 3 to 4 in the overall scheme in Figure 1. Such a pathway switch would suggest the K_D for UCGA in the absence of CUCU is near 500 μM and that there is coupling between the binding of CUCU and UCGA. This type of cooperative interaction has been suggested by McConnell et al. (1993) for the CCCUC(dU)A + G combination of substrates. The approximate K_D for UCGA of 500 μM is consistent with a limit of >200 μM obtained for rUrCdGrA by equilibrium dialysis in the presence of saturating $d(CT)_3$ at 5 mM Mg^{2+} and 5 °C (Moran et al., 1993). In addition, values of k_{cat}/K_M at 200 and 500 μM UCGA and 5 mM Mg^{2+} of 1.3×10^4 and 8.8×10^4 M^{-1} s^{-1}, respectively, are close to k_1k_2/k_{-1} measured for pyrCUCU of 5.8×10^4 M^{-1} s^{-1} in 5 mM Mg^{2+} without a 3′-splice site mimic present (Bevilacqua et al., 1992). This suggests the rate for association of CUCU with L-21 Sca I at 5 mM Mg^{2+} is not affected much by the presence of UCGA.

With 200 μM UCGA present, the k_{cat} for CUCU, corrected for fraction of ribozyme active for binding is about 3.5-fold larger in 5 than in 50 mM Mg^{2+} (Table 1). This decrease in k_{cat} with increasing Mg^{2+} is partially due to a change in the rate-limiting step, as discussed below.

Optimal 3′-Splice Site Mimic for a Model of the Second Step of Splicing. For the intron of the rRNA precursor from *T. thermophila*, base-pairing of $U^{412}C^{413}$ to $G^{313}A^{314}$ forms the P9.0 pairing that helps position the 3′-end of the intron for the second step of splicing (Michel et al., 1989; Burke et al., 1990). Sca I truncations of the ribozyme remove $U^{412}C^{413}$; consequently, these nucleotides can be added exogenously, 5′ to G, in order to form a P9.0 pairing (Figure 1) and examine their effect upon G-like substrate kinetics.

At 50 mM Mg^{2+}, steady-state kinetics were measured for GA, CGA, and UCGA reacting with 2.5 μM CUCU. Only species 2, 4, and 5 in the overall scheme in Figure 1 need be considered since [CUCU] of 2.5 μM is much larger than its expected K_D of 0.025 μM (Bevilacqua & Turner, 1991; Bevilacqua et al., 1993). Hyperbolic initial rate plots

Table 2: Steady-State Kinetic Parameters for 3′-Splice Site Mimics and L-21 Sca I at 15 °C, pH 7.4, 50 mM Hepes/25 mM Na^+

3′ splice site mimic (μM)	[Mg^{2+}] (mM)[a]	[ribozyme] (μM)	[CUCU] (μM)	K_M (μM) steady state	k_{cat} (min^{-1})[b] steady state	k_{cat}/K_M (M^{-1} s^{-1}) steady state
GA varied	50	0.125	2.5	810	0.63	13
CGA varied	50	0.125	2.5	227	1.3	98
UCGA varied	5	0.125	2.5	55	0.82	250
UCGA varied	50	0.125	2.5	5.5	0.20	610
UCGA trace	50	varied	none	>25	$\gg$0.1 (=k_{hyd})	

[a] Total ionic strength maintained at 175 mM with NaCl. [b] Data have been divided by the fraction of L-21 Sca I active under the specific salt condition (Bevilacqua & Turner, 1991) to obtain the listed *corrected* k_{cat} (see the footnote to Table 1).

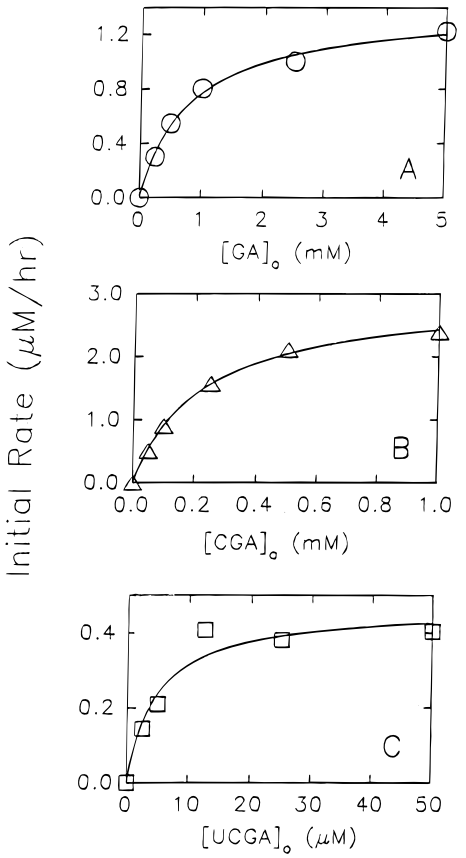

FIGURE 3: UCGA has the lowest K_M for the 3′-splice site mimics. Buffer for A−C is 50 mM Hepes (25 mM Na^+), pH 7.4, and 50 mM $MgCl_2$, with no NaCl added. All plots are of initial rate, using 2.5 μM CUCU for the 5′-exon mimic, and with 0.125 μM L-21 Sca I. (A) Plot for GA (○). k_{cat} and K_M are 0.63 min^{-1} and 810 μM, respectively. (B) Plot for CGA (△). k_{cat} and K_M are 1.3 min^{-1} and 227 μM, respectively. (C) Plot for UCGA (□). k_{cat} and K_M are 0.2 min^{-1} and 5.5 μM, respectively.

consistent with Michaelis−Menten kinetics are observed for GA, CGA, and UCGA (Figure 3). The derived kinetic constants are listed in Table 2. K_Ms for GA, CGA, and UCGA are 810, 227, and 5.5 μM, respectively. This trend is consistent with longer 3′-splice site mimics binding tighter to the ribozyme than shorter mimics and with formation of the P9.0 pairing (Burke, 1989; Moran et al., 1993).

The K_M for UCGA is larger under other conditions. At 5 mM Mg^{2+}, UCGA reacting with 2.5 μM CUCU gives a K_M of 55 μM (Table 2). In 50 mM Mg^{2+}, plots of the rate of hydrolysis of trace amounts of p*UCGA versus the concentration of L-21 Sca I are linear to 25 μM L-21 Sca I, giving a lower limit of 25 μM for a K_M for UCGA in the absence of CUCU (Table 2). These observations suggest CUCU and Mg^{2+} binding may be coupled with UCGA binding. Such

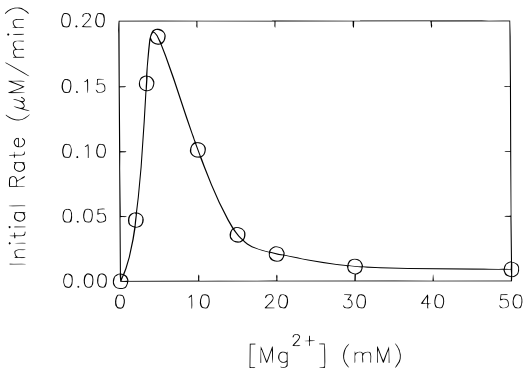

FIGURE 4: Steady-state experiments exhibit a spiked dependence on Mg^{2+}. Plot of initial rate versus [Mg^{2+}] for reaction of 2.5 μM CUCU (mixed with trace amounts of p*CUCU) and 200 μM UCGA in 0.125 μM L-21 Sca I. The difference between rates at 5, 10, and 50 mM Mg^{2+} varied among experiments, and this figure shows the experiment with the maximum differences. For all experiments, the rates at 5 and 10 mM Mg^{2+} are higher than at 50 mM Mg^{2+}. Buffer is 50 mM Hepes (25 mM Na^+), pH 7.4, with ionic strength maintained at 175 mM with NaCl. No NaCl was added at the 50 mM Mg^{2+} point.

coupled binding of substrates is consistent with UCGA aiding CUCU binding as suggested in the previous section.

At 50 mM Mg^{2+}, the k_{cat}s for GA, CGA, and UCGA are 0.63, 1.3, and 0.2 min^{-1}, respectively (Table 2). Despite having the lowest k_{cat}, UCGA has the largest specificity constant, k_{cat}/K_M = 610 M^{-1} s^{-1} (Table 2), a lower limit to the rate of UCGA binding to L-21 Sca I (Fersht, 1985). Of the 3′-splice site mimics tested, UCGA requires the lowest concentrations to obtain steady-state saturation of L-21 Sca I and fully restores the P9.0 pairing; thus, it was used as the 3′-splice site mimic in most subsequent experiments.

The Magnesium Dependence of Second Step Model Reactions Is Complex. Steady-state kinetics were measured as a function of [Mg^{2+}] for 2.5 μM CUCU reacting with 200 μM UCGA. Both substrate concentrations are saturating relative to their respective K_Ms. Enough NaCl was added at each [Mg^{2+}] to maintain a constant ionic strength of 175 mM. Under these conditions, a maximum is observed near 5 mM Mg^{2+} (Figure 4). Similar Mg^{2+} profiles are observed when [CUCU] is subsaturating at 0.04, 0.08, or 0.16 μM or when [UCGA] is raised to 500 μM (data not shown). The origin of this spiked Mg^{2+} dependence will be discussed later. This Mg^{2+} profile also occurs when the renaturation protocol of Walstrum and Uhlenbeck (1990) is used, and when the monovalent cation is K^+, Li^+, or NH_4^+ (Bevilacqua, 1993). In the presence of Li^+, however, the absolute magnitudes of the rates are reduced by about 4-fold.

Table 3: Kinetic Parameters for CUCUA, UCG, and L-21 Sca I at 15 °C, pH 7.4, 50 mM Hepes/25 mM Na^+

3′ splice site mimic (mM)	$[Mg^{2+}]$ (mM)[a]	[ribozyme] (μM)	[CUCUA] (μM)	k_{cat} (min^{-1})[b] burst	k_{rev} (min^{-1}) pulse−chase	k_{rev} (min^{-1}) single turnover	k_{rev} (min^{-1}) burst	k_{hyd} (min^{-1})	k_{off}' (min^{-1}) pulse−chase
burst									
UCG 0.2	5	1	10	0.92			>3		
UCG 0.2	50	1	10	0.003			>3		
pulse-chase									
UCG 0.2	50	10	25		>3				≈, $<k_{rev}$
single turnover									
UCG 0.2	5, 50	10	trace			>3			
none	50	10	trace					0.26	

[a] Total ionic strength maintained at 175 mM with NaCl. [b] Data have been divided by the fraction of L-21 Sca I active under the specific salt condition (Bevilacqua & Turner, 1991) to obtain the listed *corrected* k_{cat} (see the footnote to Table 1).

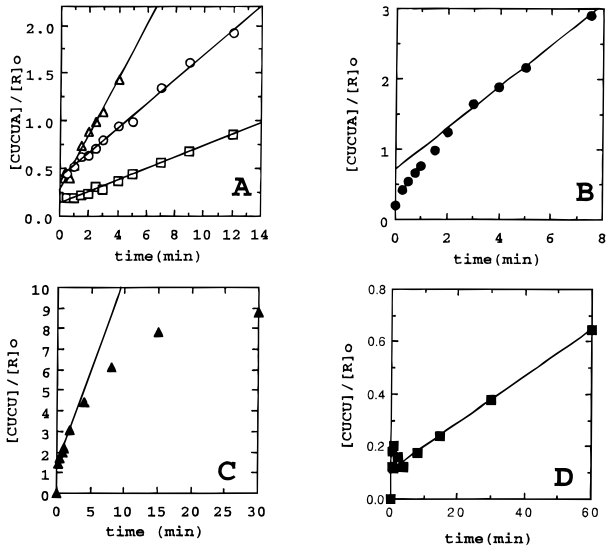

FIGURE 5: Active-site titrations reveal the fraction of L-21 Sca I able to bind substrate. Plot of number of turnovers versus time. Ribozyme concentration is initial concentration and uncorrected for improper folding (Bevilacqua & Turner, 1991). Fits are by linear least-squares to the initial part of the multiple-turnover section of the curve and extrapolated back to the *y*-axis. π, the magnitude of the burst, is the *y*-intercept of the fit (Fersht, 1985). (A) Conditions are 2.5 μM CUCU (mixed with trace amounts of p*CUCU), 0.5 μM L-21 Sca I, and 5 mM GA (○), 1 mM CGA (△), and 0.1 mM UCGA (□). Buffer is 50 mM Hepes (25 mM Na^+), pH 7.4, and 50 mM $MgCl_2$, with no NaCl added. (B) Conditions are 1.25 μM CUCU (mixed with trace amounts of p*CUCU), 0.25 μM L-21 Sca I, 0.2 mM UCGA (●). Buffer is 50 mM Hepes (25 mM Na^+), pH 7.4, 10 mM $MgCl_2$, 120 mM NaCl added. (C) Conditions are 10 μM CUCUA (mixed with trace amounts of p*CUCUA), 1 μM L-21 Sca I, and 0.2 mM UCG (▲). Buffer is 50 mM Hepes (25 mM Na^+), pH 7.4, 5.0 mM $MgCl_2$, and 135 mM NaCl. (D) Conditions as in C but buffer is 50 mM Hepes (25 mM Na^+), pH 7.4, and 50 mM $MgCl_2$, with no NaCl added (■).

Pre-Steady-State Kinetics

Description of Active-Site Titrations. Active-site titrations were performed with limiting amounts of L-21 Sca I (0.125−1 μM), 5−20-fold excess of CUCU with trace amounts of 5′-^{32}P labeled CUCU, and large excess of GA, CGA, or UCGA. Both oligomers were added simultaneously to L-21 Sca I. These conditions were chosen so that >1 turnover occurs, but the first turnover gives 5−20% reaction and is thus observable. Analogous concentrations of CUCUA and UCG were chosen for active-site titrations for the reverse reaction (see appropriate table). The first turnover occurs at a rate k_{for} and subsequent turnovers at a rate k_{cat} given by Eq 2 (also see steady-state scheme in Figure 2). The size of any burst, π, is given in eq 4 (Fersht, 1985).

$$\pi = \left(\frac{k_{for}}{k_{for} + k_{release}}\right)^2 \frac{[R]_{active}}{[R]_o} \quad (4)$$

Thus k_{cat} is given by the slope of the multiple turnover portion of the plots shown in Figure 5 (Fersht, 1985).

Active-Site Titrations at 5, 10, and 50 mM Mg^{2+} for the Forward Reaction. Active-site titrations were performed for the forward reaction at 5, 10, and 50 mM Mg^{2+} with GA, CGA, and UCGA. There is no burst at 5 mM Mg^{2+}. This suggests that $k_{for} \ll k_{release}$ and $k_{cat} = k_{for}$ at 5 mM Mg^{2+}. At 50 mM Mg^{2+}, however, rapid bursts are observed (Figure 5A). With GA, CGA, and UCGA, π is 0.4, 0.3, and 0.2, respectively (Figure 5A). The burst of 0.2 with UCGA is found for L-21 Sca I concentrations of both 0.25 and 0.5 μM, when [CUCU] is 1.25 and 2.5 μM, respectively. Limits for k_{for} and values for k_{cat} provided from the first and subsequent turnovers, respectively, are listed in Table 1. Equilibrium dialysis experiments indicate that only 30% of the ribozyme population binds CUCU tightly at 50 mM Mg^{2+} in the presence of 5 mM pdG (Bevilacqua & Turner, 1991). The simplest interpretation of the burst experiments is that at 50 mM Mg^{2+} most of the ribozyme population with CUCU tightly bound is reactive and that $k_{for} \gg k_{release}$ and $k_{cat} = k_{release}$. The somewhat smaller burst with UCGA may be due to a preference for the order of substrate addition under these conditions (see single-turnover results) or may indicate that not every CUCU·L-21 Sca I·UCGA complex leads to reaction at 50 mM Mg^{2+}.

A burst is also seen with CUCU and UCGA at 10 mM Mg^{2+} (Figure 5B). Unlike the burst at 50 mM Mg^{2+}, the burst at 10 mM Mg^{2+} is not instantaneous. Nevertheless, the presence of a burst at 10 mM Mg^{2+} suggests $k_{for} \geq k_{release}$.

Active-Site Titrations at 5 and 50 mM Mg^{2+} for the Reverse Reaction. Active-site titrations were also performed for the reverse reaction at 5 and 50 mM Mg^{2+}. For reaction of CUCUA with UCG, bursts of 1.2 and 0.2 are observed at 5 and 50 mM Mg^{2+}, respectively (Figures 5C,D). Limits for k_{rev} and values for k_{cat} provided from the first and subsequent turnovers, respectively, are listed in Table 3. Equilibrium dialysis experiments indicate all of the ribozyme is active for binding CUCU tightly at 5 mM Mg^{2+} (Bevilacqua & Turner, 1991). The simplest interpretation of these observations is that $k_{rev} \gg k_{-release}$ and $k_{cat} = k_{-release}$ at 5 mM Mg^{2+}, and that the entire ribozyme population is reactive.

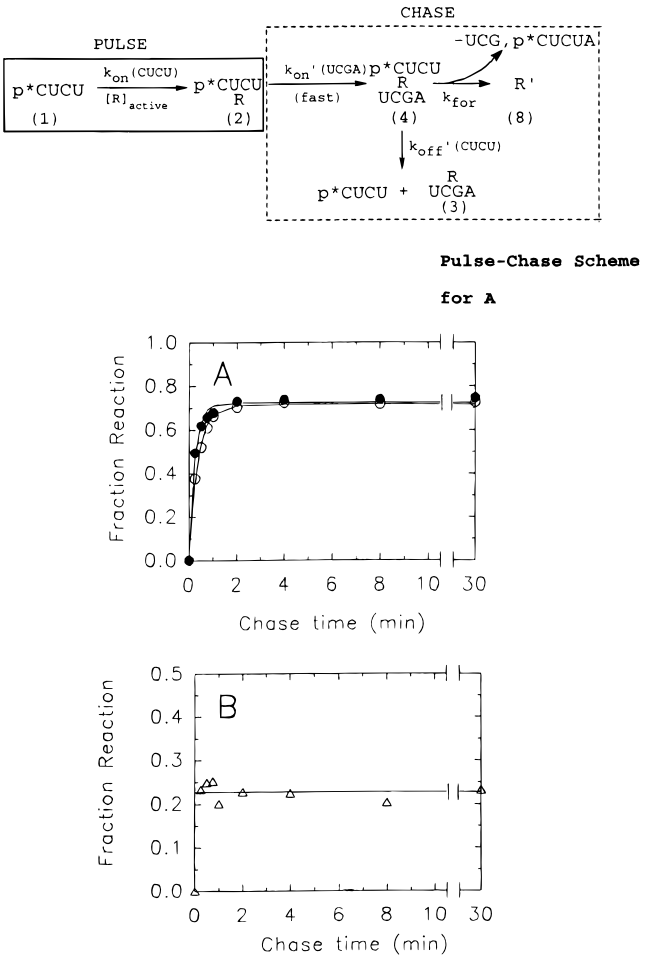

FIGURE 6: Pulse−chase experiments. On top is the pulse-chase scheme corresponding to reaction with p*CUCU in panel A. Steps relevant to the pulse portion of the experiment are enclosed in a solid box, and steps relevant to the chase portion of the experiment are enclosed in a dashed-line box. Panels A and B show plots of fraction reaction versus time after addition of the chase. (A) Fraction reaction is defined as [p*CUCUA]/([p*CUCU] + [p*CUCUA]), corresponding to the pulse-chase scheme shown at top. Pulse is 2.5 μM L-21 Sca I and trace amounts of p*CUCU in a volume of 3 μL. Pulse is allowed to incubate at 15 °C for 1 min. Chase is 27 μL of 25 μM CUCU and 200 μM UCGA (equilibrated for at least 5 min at 15 °C before addition to the pulse). Buffer is 50 mM Hepes (25 mM Na^+), pH 7.4, with 10 mM Mg^{2+} and 120 mM NaCl (○), or 50 mM Mg^{2+} no added NaCl (●). (B) Fraction reaction is defined as [p*CUCU]/([p*CUCU] + [p*CUCUA]). Pulse−chase kinetics were done in two steps, similar to the method of Herschlag and Cech (1990). Pulse is 10 μM L-21 Sca I and trace amounts of p*CUCUA in a volume of 3 μL. Pulse is allowed to incubate at 15 °C for 1 min. Chase is 27 μL of 25 μM CUCUA and 200 μM UCG (equilibrated for at least five minutes at 15 °C before addition to the pulse). Buffer is 50 mM Hepes (25 mM Na^+), pH 7.4, and 50 mM Mg^{2+} with no added NaCl (△) .

($k_{-\text{release}}$ includes all CUCU and UCGA release steps and any conformational changes of the ribozyme at rate $k_{-\text{conf}}$.) In contrast, the burst of 0.2 at 50 mM Mg^{2+} is consistent with the active-site titration of the forward reaction and equilibrium dialysis results on CUCU at 50 mM Mg^{2+} (Bevilacqua & Turner, 1991) and indicates that only about 20% of the ribozyme binds CUCUA or CUCU in a productive complex. It also indicates that, at 50 mM Mg^{2+}, the rate-limiting step is after chemistry for both directions of the reaction.

Description of Pulse−Chase Trapping Experiments. The pulse-chase scheme for CUCU is shown in Figure 6. Similar schemes can be derived for 3′-splice site mimics. Two equations apply during the chase:

$$\tau^{-1} = k_{\text{for}} + k_{\text{off}}'(\text{CUCU}) \quad (5)$$

$$F = k_{\text{for}}/(k_{\text{for}} + k_{\text{off}}'(\text{CUCU})) \quad (6)$$

where τ^{-1} is the rate, and F is the fraction of p*CUCU trapped at equilibrium. For CUCU, k_{off} is limited by the rate of P1 dissociation from the catalytic core, k_{-2} (Bevilacqua et al., 1992).

To allow interpretations of pulse-chase experiments, several conditions must be met:

Condition (1). The pulse time must be long enough to allow p*CUCU binding to reach equilibrium. Stopped-flow experiments in 5 mM Mg^{2+} for pyrCUCU binding to L-21 Sca I provide k_{on} and k_{off} of 5.8 x 10^4 M^{-1} s^{-1} and 0.076 s^{-1}, respectively (Bevilacqua et al., 1992). Assuming the same rates at 50 mM Mg^{2+} and correcting the L-21 Sca I concentration for the 70% that is inactive at 50 mM Mg^{2+} (Bevilacqua & Turner, 1991) suggests trace amounts of p*CUCU should bind to an initial concentration of 2.5 μM L-21 Sca I with a $t_{1/2}$ of 10 s. With 2.5 μM L-21 Sca I present, the length of the pulse was varied from 15 s to 10 min. Maximal trapping is observed for pulse times 30 s and longer, and about two-thirds maximal trapping is observed after a 15 s pulse, consistent with the prediction from pyrCUCU experiments. All subsequent pulse−chase experiments were thus performed with a 1 min pulse. Apparently the rate at which CUCU binds to L-21 Sca I is similar at both 5 and 50 mM Mg^{2+}.

Condition (2). During the pulse, [L-21 Sca I] must be large enough to bind all the p*CUCU. Under the above conditions, the [L-21 Sca I] in the pulse was varied from 2.5 to 10 μM in 50 mM Mg^{2+}. The amount of p*CUCU trapped is 60−70% for all of these L-21 Sca I concentrations. This indicates that the K_D at 50 mM Mg^{2+} for CUCU binding to the 30% active L-21 Sca I is <0.75 μM (2.5 μM × 0.3). This is consistent with the expected K_D of 0.025 μM (Bevilacqua & Turner, 1991; Bevilacqua et al., 1993). All subsequent pulse−chase experiments were thus performed with 2.5 μM L-21 Sca I in the pulse.

Condition (3). During the chase, the [UCGA] must be large enough that its binding is rapid and UCGA binds all the L-21 Sca I before p*CUCU dissociates. Under the above conditions, the [UCGA] in the chase was varied from 50 to 500 μM in 50 mM Mg^{2+}. The amount of p*CUCU trapped is unchanged for all of these chases. This indicates that 50 μM UCGA is sufficient to provide maximal trapping. All subsequent pulse−chase experiments were performed with 200 μM UCGA in the chase.

Condition (4). During the chase, the [CUCU] must be large enough that dissociation of p*CUCU is essentially irreversible. Under the above conditions, concentrations after the chase are ≈1 nM p*CUCU, ≈25 μM CUCU, ≈200 μM UCGA, and 0.25 μM L-21 Sca I. To determine whether 25 μM CUCU is sufficient to make p*CUCU dissociation effectively irreversible, 29 μL of ≈25 μM CUCU, ≈200 μM UCGA, and 0.25 μM L-21 Sca I was mixed for 5 min prior to addition of 1 μL of trace amounts of p*CUCU in 50 mM Mg^{2+}. The rate of relaxation for this case is slow, taking 30 min to give 5% product and over 24 h to come to completion. p*CUCU dissociation can thus be considered essentially irreversible for these experiments.

Pulse−Chase Experiments at 5, 10, and 50 mM Mg^{2+} for CUCU. Using appropriate conditions determined from the above experiments, trapping was examined with CUCU at 5, 10, and 50 mM Mg^{2+} (pulse−chase scheme in Figure 6). Sixty to seventy percent trapping is observed at 10 and 50 mM Mg^{2+} with an L-21 Sca I concentration of 2.5 μM during a 1 min pulse and 25 μM CUCU and 200 μM UCGA in the chase (Figure 6A). The rate of relaxation, τ^{-1}, at 10 and 50 mM Mg^{2+} is similar at about 2.8 min^{-1} (Table 1). At 5 mM Mg^{2+}, under identical conditions, no trapping is observed. Clearly, there is a striking change in trapping behavior between 5 and 10 mM Mg^{2+}.

In addition to measuring p*CUCU trapping in chases with UCGA, trapping was measured for 5 mM GA and 1 mM CGA chases in 50 mM Mg^{2+}. As with UCGA, trapping of p*CUCU is about 60% in GA and CGA chases. The rate of trapping is faster for a CGA chase than a GA or UCGA chase, however. For the CGA chase, $\tau^{-1} \gg 3$ min^{-1} versus $\tau^{-1} = 2.8$ min^{-1}, for GA and UCGA chases. Similar trapping results were found for a 10 mM GA chase. Taken together, the above observations lead to two possible interpretations.

Case 1. Only 60−70% of ribozyme bound with p*CUCU at 10 and 50 mM Mg^{2+} (species 2 in the pulse−chase scheme in Figure 6) is capable of carrying out chemistry. If so, the observed 60−70% trapping actually represents complete trapping of p*CUCU (i.e., $k_{for} = 1/\tau \gg k_{off}'$(CUCU)). It is clear that high concentrations of Mg^{2+} induce some unusual properties of L-21 Sca I since 50 mM Mg^{2+} leads to 70% of L-21 Sca I being folded incorrectly for binding CUCU (Bevilacqua & Turner, 1991). Under the conditions of the pulse−chase experiment, however, this still leaves a large excess of L-21 Sca I for binding p*CUCU. Thus of the approximately 30% excess ribozyme remaining active for binding p*CUCU, 30−40% may not bind G-substrate productively.

Case 2. All of species 2 is active, and less than 100% trapping is observed because $k_{for} \approx 2k_{off}'$(CUCU).

We favor case 1 since the faster forward rate with CGA chase does not lead to increased fraction reaction, although we cannot rule out a fortuitous increase in k_{off}'(CUCU) induced by CGA binding. Thus, limiting values for k_{for} and k_{off}'(CUCU) consistent with both cases will be presented. Using limits does not severely compromise interpretation of trapping results since several useful quantitative and qualitative conclusions are still readily apparent for CUCU: (1) Trapping in 10 and 50 mM Mg^{2+} is similar, indicating that, with UCGA present, k_{for} is 1.8−2.8 min^{-1} and k_{off}'(CUCU) $\leq$ 1.0 min^{-1} at high [Mg^{2+}] (similar values of k_{for} and k_{off}'(CUCU) are obtained with a GA chase); (2) trapping in 50 mM Mg^{2+} indicates that, with CGA present, $k_{for} > 3$ min^{-1} and k_{off}'(CUCU) $\leq k_{for}$; and (3) absence of trapping in 5 mM Mg^{2+} indicates that, with UCGA present, k_{off}'(CUCU) $\gg k_{for}$ at 5 mM Mg^{2+}. Clearly there is a large change in the relative values of k_{off}'(CUCU) and k_{for} between 5 and 10 mM Mg^{2+} (see Discussion).

Pulse−Chase Trapping Experiments at 5 and 50 mM Mg^{2+} for CUCUA. Trapping was examined with CUCUA at 5 and 50 mM Mg^{2+}. During the pulse, p*CUCUA was preincubated in 10 μM L-21 Sca I for 1 min, and 25 μM CUCUA and 200 μM UCG were added in the chase. (Control experiments indicate that <20% hydrolysis of p*CUCUA occurred during this pulse, and this is subtracted from observed trapping.) As with CUCU, trapping of CUCUA is present at 50 mM Mg^{2+}, but absent at 5 mM Mg^{2+}. The extent of trapping at 50 mM Mg^{2+} is approximately 25%, and relaxation is instantaneous (i.e., $t_{1/2} \ll 15$ s, the shortest time point acquired; Figure 6B). These observations lead to two conclusions for CUCUA: (1) At 50 mM Mg^{2+}, $k_{rev} > 3$ min^{-1} and k_{off}'(CUCUA) $\approx k_{rev}$ (Table 3), and (2) at 5 mM Mg^{2+}, k_{off}'(CUCUA) $\gg k_{rev}$. Under conditions of 5 mM Mg^{2+} and 15 °C but in the absence of UCG, experiments with 5′-pyrene (pyr) labeled CUCUA indicate that pyrCUCUA is undocked and essentially never in the catalytic site (Bevilacqua et al., 1994), consistent with an absence of p*CUCUA trapping at 5 mM Mg^{2+}. Thus, similar to CUCU there is a large change in the relative values of k_{off}(CUCUA) and/or k_{rev} between 5 and 50 mM Mg^{2+}.

The trapping of CUCUA for a hydrolysis reaction was also measured at 50 mM Mg^{2+}. During the pulse, p*CUCUA was preincubated in 10 μM L-21 Sca I for 1 min, and 25 μM CUCUA *only* was added in the chase. After correction for the < 20% hydrolysis of p*CUCUA occurring during the pulse, no trapping of p*CUCUA by hydrolysis is observed. This indicates that, at 50 mM Mg^{2+} in the absence of UCG, k_{off}(CUCUA) $\gg k_{hyd}$. A single-turnover reaction for hydrolysis of trace amounts of p*CUCUA with 10 μM L-21 Sca I was measured at 50 mM Mg^{2+} to obtain k_{hyd}. The rate of the single-turnover hydrolysis reaction, k_{hyd}, is 0.26 min^{-1} (Table 3). This observation in combination with the absence of trapping for the CUCUA hydrolysis reaction indicates that k_{off}(CUCUA) $\gg$ 0.26 min^{-1}.

Description of Single-Turnover/Order-of-Addition Reactions. Single-turnover kinetics for the forward reaction were measured with trace amounts of p*CUCU, 2.5 μM L-21 Sca I, and 200 μM UCGA. These conditions ensure that only one turnover of CUCU is possible and that binding of CUCU is rapid and complete. The order of addition of reactants was varied in different experiments. Analogous concentrations of CUCUA and UCG were chosen for the single-turnover experiments of the reverse reaction as listed in the appropriate table. Single-turnover schemes for the forward reaction are shown in Figure 7. Similar schemes can be derived for the reverse reaction.

Single-Turnover/Order-of-Addition Experiments at 5 and 50 mM Mg^{2+} for the Forward Reaction. Single-turnover results are sensitive to the addition order of substrates at 50 mM Mg^{2+}, but not at 5 mM Mg^{2+}. As shown in Figure 7, single-turnover reactions in 50 mM Mg^{2+} are considerably faster if p*CUCU is added to the ribozyme first. The rate constants, k_{st}, observed for first-addition of p*CUCU and UCGA are 1.1 and 0.16 min^{-1}, respectively (Table 1), and first addition of UCGA may produce a kinetic lag (Figure 7). The observed rate for single-turnover reactions initiated by pathway (I) at 50 mM Mg^{2+} is consistent with k_{for}. At 50 mM Mg^{2+}, CUCU apparently binds slowly in the presence of UCGA, or CUCU must bind before UCGA to give a productive complex. Interestingly, in intron splicing, a CUCU exon end is generated before UCGA enters the catalytic site. Simultaneous addition of both substrates to L-21 Sca I gives an intermediate rate, $k_{st} = 0.31$ min^{-1}.

Single-Turnover/Order-of-Addition Experiments at 5 and 50 mM Mg^{2+} for the Reverse Reaction. Single-turnover kinetics were also examined for the reverse reaction at 5 and 50 mM Mg^{2+}. When L-21 Sca I is preincubated with UCG, single-turnover is rapid at both 5 and 50 mM Mg^{2+} (Table 3). This observation is consistent with rapid trapping

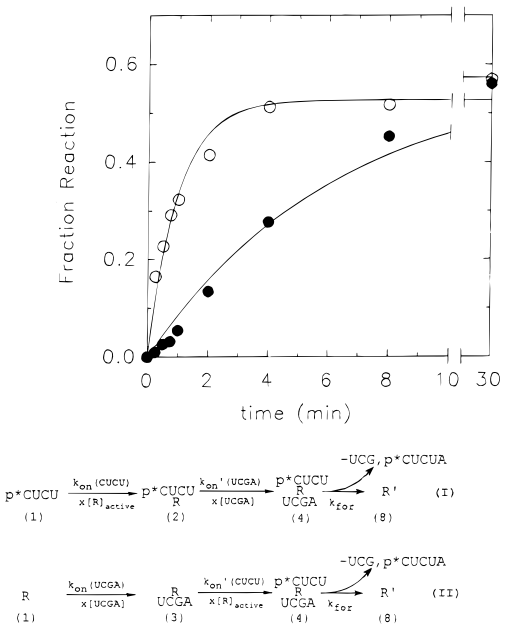

FIGURE 7: Order-of-addition experiments. Plot of fraction reaction versus time. Fraction reaction is defined as [p*CUCUA]/([p*CUCU] + [p*CUCUA]). A 4×UCGA solution (800 μM UCGA) in reaction buffer, a 4×p*CUCU solution (trace amounts of p*CUCU) in reaction buffer, and a 2× L-21 Sca I solution (5 μM L-21 Sca I) in reaction buffer were prepared and allowed to equilibrate separately for at least 5 min at 15 °C. (●) 10 μL of 4×UCGA was preincubated with 20 μL of 2× L-21 Sca I for 10 min followed by addition of 10 μL of 4×p*CUCU. Shown are the fits to single-exponential equations. The fit for the UCGA-preincubation experiment is poor because the initial lag is not considered in the exponential equations. (○) 10 μL of 4×p*CUCU was preincubated with 20 μL of 2× L-21 Sca I for 10 min followed by addition of 10 μL of 4×UCGA. Reaction buffer is 50 mM Hepes (25 mM Na^+), pH 7.4, and 50 mM $MgCl_2$, with no NaCl added. Shown also are the single-turnover schemes for the forward reaction. In scheme I, L-21 Sca I and p*CUCU are preincubated followed by addition of UCGA. In scheme II, L-21 Sca I and UCGA are preincubated followed by addition of p*CUCU. In other single-turnover experiments, both p*CUCU and UCGA are added simultaneously. Pathway I is identical to that followed in pulse−chase experiments where binding of UCGA and CUCU are known to be fast; thus, the rate of single-turnover is predicted to be k_{for}. In pathway II no partitioning was observed by pulse−chase experiments, and so a simple rate cannot be predicted.

when CUCUA is preassociated with L-21 Sca I at 50 mM Mg^{2+} and with rapid burst kinetics at 5 and 50 mM Mg^{2+} (Table 3). Evidently, the preference for preassociation of 5′-exon mimic with L-21 Sca I for the forward reaction is absent for the reverse reaction, or UCG does not impede the reverse reaction enough to bring its rate under the 3 min^{-1} measurable by methods employed here. It is also possible, however, that UCG can impede the reverse reaction but that its dissociation from the ribozyme is more rapid than that of UCGA, though this is unlikely.

DISCUSSION

The results reported here help define a model system for studies of the second step of splicing, i.e., exon ligation, and for reverse cyclization (Cech, 1990). Substrates are identified that obey Michaelis−Menten kinetics and allow rate saturation to be achieved at micromolar concentrations with formation of the P9.0 pairing important for positioning the 3′-splice site for the second step of splicing. An unusual dependence of rate on [Mg^{2+}] is explained. The position of the rate-limiting step in the overall mechanism is identified relative to chemistry. The results provide the foundation for additional equilibrium and pre-steady-state experiments, some of which have already been reported (Bevilacqua et al., 1994). The temperature of 15 °C is convenient for such experiments since it is slightly below room temperature where evaporation of solvent is not a problem. Moreover, it is roughly in the middle of the viable temperature range for *Tetrahymena* (Bick, 1972).

CUCU and UCGA Are the Best Minimal-Length Substrates That Obey Michaelis−Menten Kinetics. CU and UCU provided well-behaved substrates for reverse-cyclization experiments with the circular form of the group I intron (Sugimoto et al., 1988). Neither provides simple steady-state kinetics with L-21 Sca I, however. CU gives cooperative concentration dependence of steady-state kinetics (Figure 2A) suggesting at least two CUs must bind to give reaction. Allowing G·U pairs, a single CU could potentially base-pair at four different positions on the internal guide sequence (Figure 1). Perhaps binding to each of these sites individually is either weak, nonreactive, or both. Interestingly, a single CU appears able to induce the circle opening reaction of this intron (Sugimoto et al., 1988). In this case, however, placement of the reactive CU on the IGS is shifted such that a neighboring CU cannot form base pairs (Been & Cech, 1987; Sugimoto et al., 1988).

UCU is not a good substrate for kinetic studies because it inhibits reaction before rate saturation is achieved. This could be due to the binding of two UCU molecules to the IGS to give a P1 helix that docks unproductively in the catalytic core or binding of UCU to another site that is inhibitory.

Steady-state kinetics with CUCU follow Michaelis−Menten behavior (Figure 2C). Thus, CUCU is the minimal-length 5′-exon mimic that is suitable for detailed kinetic studies.

All three 3′-splice site mimics tested, GA, CGA, and UCGA, obey Michaelis−Menten kinetics with UCGA having the lowest K_M and highest k_{cat}/K_M. Thus, UCGA appears to form the P9.0 pairing important for second step splicing models and provides a suitable 3′-splice site mimic for detailed kinetic studies. The change in K_M^{CUCU} with UCGA concentration (Table 1) and of K_M^{UCGA} with CUCU concentration (Table 2) suggests coupling between UCGA and CUCU binding of 0.9−1.5 kcal/mol. This is consistent with that observed by McConnell et al. (1993) for CCCUC(dU)A and G. Thus it appears that coupling occurs between substrates for reactions mimicking both the first and second steps of splicing. The coupled binding of UCGA and CUCU would favor the second step of splicing over biologically unproductive 3′-splice site hydrolysis in the natural intron.

While UCGA has the lowest K_M and highest k_{cat}/K_M of the 3′-splice site mimics tested, CGA has the largest k_{cat}. At 50 mM Mg^{2+} k_{cat} for CGA is 1.3 min^{-1} versus 0.63 min^{-1} and 0.20 min^{-1} for GA and UCGA (Table 2). A CGA chase also gives a faster k_{for} in single-turnover pulse−chase experiments with p*CUCU (≫3 min^{-1} versus 2.8 min^{-1} for GA and UCGA). Thus, accelerated reaction with CGA is present under both multiple- and single-turnover kinetics. G is held in the ribozyme active site by a base triple (Michel et al., 1989; Yarus et al., 1991). Because ribozyme-bound CGA forms only one Watson−Crick base pair, C to G^{313}, it is unlikely that bound CGA has any extensive double-helical

character. The additional base pair formed by ribozyme-bound UCGA, U to A^{314}, however, creates a two-base-pair section of double helix. This could inhibit optimal orientation at the active site.

All the Ribozyme Is Active at 5 mM Mg^{2+} but not at 50 mM Mg^{2+}. Scatchard plots at 5 mM Mg^{2+} indicate that the entire ribozyme population is capable of binding CUCU in a 1:1 stoichiometry (Bevilacqua & Turner, 1991). The presence of a complete burst for the reverse reaction at 5 mM Mg^{2+} indicates that all of the ribozyme is also active for binding CUCUA and UCG and for catalyzing reaction.

Scatchard plots at 50 mM Mg^{2+} indicate 30% of the ribozyme binds CUCU tightly (Bevilacqua & Turner, 1991). This is consistent with the presence of bursts, $\pi \approx 0.2-0.4$, for both forward and reverse reactions at 50 mM Mg^{2+}, suggesting approximately 30% of L-21 Sca I is active. The results suggest that most but perhaps not all the ribozyme population capable of binding CUCU can also bind the 3′-splice site mimic and catalyze reaction. Since the burst of $\pi \approx 0.2-0.4$ is observed for both the forward and reverse reactions, it is likely that CUCUA does not distinguish between the two ribozyme populations any differently than CUCU.

The Rate-Limiting Step Changes between 5 and 10 mM Mg^{2+} for the Forward Direction. For the Reverse Direction, It Is after Chemistry at Both 5 and 50 mM Mg^{2+}. At 5 mM Mg^{2+}, the absence of a burst for the forward reaction indicates the rate-limiting step is k_{for}, representing chemistry or steps before chemistry or a combination of both. At 50 mM Mg^{2+}, the presence of a stoichiometric burst indicates the rate-limiting step for multiple turnover is after chemistry for the forward reaction. Thus, as $[Mg^{2+}]$ is increased from 5 to 50 mM the step limiting k_{cat} in the forward direction of the overall scheme in Figure 1 switches from k_{for} to $k_{release}$. ($k_{release}$ is a combination of product dissociation and k_{conf}, as defined in the steady-state scheme in Figure 2.)

For the reverse reaction, stoichiometric bursts are observed at both 5 and 50 mM Mg^{2+}, indicating the rate-limiting step for multiple turnover in the reverse direction is after chemistry for both 5 and 50 mM Mg^{2+}. The limiting rate could be k_{-conf}, product dissociation, or a combination of both. Thus, these experiments suggest the existence of conformational changes that may limit multiple-turnover of the ribozyme.

Implications for Mg^{2+} Dependence of Various Rates. Since no burst occurs in the forward direction at 5 mM Mg^{2+}, $k_{for} = k_{cat} \approx 0.8$ min^{-1} (Table 1). Pulse−chase and burst experiments show that k_{for} is between 1.8 and 2.8 min^{-1} at 10 or 50 mM Mg^{2+} (Table 1). Thus, k_{for} *increases* with increasing $[Mg^{2+}]$.

Since CUCU does not trap at 5 mM Mg^{2+}, k_{off}'(CUCU) $\gg k_{for}$ (0.8 min^{-1}). This implies that at 5 mM Mg^{2+} k_{off}'(CUCU) is ≥ 3 min^{-1}. The measured value of k_{off}(CUCU) from stopped-flow experiments is 3 min^{-1} (Bevilacqua et al., 1993). Pulse−chase experiments show that k_{off}'(CUCU) ≤ 1.0 min^{-1} at 10 or 50 mM Mg^{2+} (Table 1). Thus, k_{off}'(CUCU) *decreases* with increasing $[Mg^{2+}]$. Apparently, the dual effects of increased $[Mg^{2+}]$ on increasing k_{for} and decreasing k_{off}'(CUCU) are responsible for the onset of trapping at 10 mM Mg^{2+}. These effects suggest the existence of Mg^{2+} binding sites near CUCU with K_Ds on the order of 10 mM. Occupancy of these binding sites by Mg^{2+} could increase k_{for} and decrease k_{off}'(CUCU).

The dependence of k_{cat} on $[Mg^{2+}]$ at 2.5 μM CUCU and 200 μM UCGA is sharply spiked (Figure 4). k_{cat} as defined and measured here increases as k_{for}, $k_{release}$, and $[R]_{active}$. As stated above, as $[Mg^{2+}]$ increases, k_{for} increases, but $k_{release}$ and the fraction of active L-21 Sca I decrease. Because $k_{release}$ (10 or 50 mM Mg^{2+}) < k_{for}(5 mM Mg^{2+}), the negative effect of high $[Mg^{2+}]$ on $k_{release}$ overwhelms the stimulatory effect of high $[Mg^{2+}]$ on k_{for} and causes a spiked profile. The incorrect folding of ribozyme at high $[Mg^{2+}]$ accentuates the spiked effect by leaving only a fraction of L-21 Sca I active for binding (Bevilacqua & Turner, 1991).

Implications for the Undocking of P1. One advantage of using the short oligonucleotide substrates presented here is that their off-rates are not limited by helix dissociation. Studies show that CUCU dissociates from ribozyme in two steps: undocking followed by breaking of base pairs (Bevilacqua et al., 1992). The rate for CUCU dissociation, however, is limited by the rate of undocking, k_{-2}, since breaking base pairs is rapid for this short substrate. Experiments performed here allow several conclusions to be made regarding k_{-2}:

(1) Binding of GA, CGA, and UCGA does not require undocking of P1 from the catalytic core. Pulse−chase experiments with p*CUCU in 10 or 50 mM Mg^{2+} lead to 60−70% trapping of p*CUCU with GA, CGA, and UCGA in the chase. This result establishes that 3′-splice site mimic binds before CUCU dissociates from the free ribozyme. Since dissociation of CUCU from the ribozyme is limited by the rate of P1 undocking, k_{-2}(CUCU), trapping of CUCU implies that GA, CGA, and UCGA are able to diffuse into the G-binding site, bind, and promote chemistry in the presence of a *docked* P1 helix. This sequence would favor a smooth progression from the first to the second step of splicing in the natural intron, since the UCGU sequence could be immediately assembled with the docked P1 helix generated by the first step of splicing. The converse of this sequence may not be possible at high $[Mg^{2+}]$. Single-turnover experiments at 50 mM Mg^{2+} show a lag and slower kinetics when UCGA binds prior to CUCU. This is a sequence that would occur in the natural intron only if P1 undocked after the first step of splicing and before UCGU assembled with the catalytic core. Thus the structure of the RNA at high Mg^{2+} appears to favor the ordered series of assembly steps required for the two steps of splicing.

(2) k_{-2}'(CUCU) decreases sharply between 5 and 10 mM Mg^{2+} (see above). Undocking of CUCU from the free ribozyme is consistent with one-step breaking of tertiary contacts between P1 and the catalytic core (Bevilacqua et al., 1992). Assuming this mechanism for CUCU dissociation is still true in the presence of UCGA, the decrease in k_{-2}'(CUCU) when $[Mg^{2+}]$ is raised from 5 to 10 mM suggests the ribozyme tertiary structure holding P1 into the catalytic core is stabilized by cooperative binding of Mg^{2+} ion(s) with apparent K_Ds of 5−10 mM. Association of Mg^{2+} counterions with ribozyme upon docking is also consistent with docking being driven by a favorable entropy change (Li et al., 1995), and with the observation that the interaction of several nonbridging phosphate oxygens with Mg^{2+} is important for splicing (Christian & Yarus, 1993).

The results here provide the basis for design of pre-steady-state rapid-reaction experiments to isolate individual kinetic

steps (Bevilacqua et al., 1994). The results presented above raise several questions that can be resolved by such experiments.

ACKNOWLEDGMENT

We thank Kevin Weeks for critically reading the manuscript and Sean Moran for the gift of UCG.

REFERENCES

Been, M. D., & Cech, T. R. (1987) *Cell 50*, 951−961.
Bevilacqua, P. C. (1993) Ph.D. Thesis, University of Rochester, Rochester, NY.
Bevilacqua, P. C., & Turner, D. H. (1991) *Biochemistry 30*, 10632−10640.
Bevilacqua, P. C., Kierzek, R., Johnson, K. A., & Turner, D. H. (1992) *Science 258*, 1355−1358.
Bevilacqua, P. C., Johnson, K. A., & Turner, D. H. (1993) *Proc. Natl. Acad. Sci. U.S.A. 90*, 8357−8361.
Bevilacqua, P. C., Li, Y., & Turner, D. H. (1994) *Biochemistry 33*, 11340−11348.
Bick, H. (1972) *Ciliated Protozoa*, p 74, World Health Organization, Geneva.
Borer, P. N. (1975) in *Handbook of Biochemistry and Molecular Biology: Nucleic Acids* (Fasman G. D., Ed.) 3rd ed., Vol. I, p 597, CRC Press, Cleveland, OH.
Burke, J. M. (1989) *FEBS Lett. 250*, 129−133.
Burke, J. M., Esherick, J. S., Burfeind, W. R., & King, J. L. (1990) *Nature 344*, 80−82.
Cech, T. R. (1990) *Annu. Rev. Biochem. 59*, 543−568.
Cech, T. R., Herschlag, D., Piccirilli, J. A., & Pyle, A. M. (1992) *J. Biol. Chem. 267*, 17479−17482.
Cech, T. R., Damberger, S. H., & Gutell, R. R. (1994) *Nature Struct. Biol. 1*, 273−280.
Celander, D. W., & Cech, T. R. (1991) *Science 251*, 401−407.
Christian, E. L., & Yarus, M. (1993) *Biochemistry 32*, 4475−4480.
Fersht, A. (1985) *Enzyme Structure and Mechanism*, 2nd ed., W. H. Freeman, New York.
Herschlag, D. (1992) *Biochemistry 31*, 1386−1399.
Herschlag, D., & Cech, T. R. (1990) *Biochemistry 29*, 10159−10171.
Herschlag, D., & Khosla, M. (1994) *Biochemistry 33*, 5291−5297.
Herschlag, D., Eckstein, F., & Cech, T. R. (1993a) *Biochemistry 32*, 8299−8311.
Herschlag, D., Eckstein, F., & Cech, T. R. (1993b) *Biochemistry 32*, 8312−8321.
Inoue, T., & Kay, P. S. (1987) *Nature 327*, 343−346.
Johnson, K. A. (1992) in *The Enzymes* (Sigman, D., Ed.) Vol. 20, p 1−61, Academic Press, New York.
Kierzek, R., Caruthers, M. H., Longfellow, C. E., Swinton, D., Turner, D. H., & Freier, S. M. (1986) *Biochemistry 25*, 7840−7846.
Kim, S. -H., & Cech, T. R. (1987) *Proc. Natl. Acad. Sci. U.S.A. 84*, 8788−8792.
Li, Y., Bevilacqua, P. C., Mathews, D., & Turner, D. H. (1995) *Biochemistry 34*, 14394−14399.
Longfellow, C. E., Kierzek, R., & Turner, D. H. (1990) *Biochemistry 29*, 278−285.
McConnell T. S., & Cech, T. R. (1995) *Biochemistry 34*, 4056−4067.
McConnell T. S., Cech, T. R., & Herschlag, D. (1993) *Proc. Natl. Acad. Sci. U.S.A. 90*, 8362−8366.
Michel, F., Hanna, M., Green, R., Bartel, D., & Szostak, J. W. (1989) *Nature 342*, 391−395.
Michel, F., Netter, P., Xu, M.-Q., & Shub, D. A. (1990) *Genes Dev. 4*, 777−788.
Moran, S., Kierzek, R., & Turner, D. H. (1993) *Biochemistry 32*, 5247−5256.
Narlikar, G. J., Gopalakrishnan, V., McConnell, T. S., Usman, N., & Herschlag, D. (1995) *Proc. Natl. Acad. Sci. U.S.A. 92*, 3668−3672.
Piccirilli, J. A., Vyle, J. S., Caruthers, M. H., & Cech, T. R. (1993) *Nature 361*, 85−88.
Price, J. V., & Cech, T. R. (1988) *Genes Dev. 2*, 1439−1447.
Pyle, A. M., & Cech, T. R. (1991) *Nature 350*, 628−631.
Richards, E. G. (1975) in *Handbook of Biochemistry and Molecular Biology: Nucleic Acids* (Fasman, G. D., Ed.) 3rd ed., Vol. I, p 597, CRC Press, Cleveland, OH.
Sugimoto, N., Kierzek, R., & Turner, D. H. (1988) *Biochemistry 27*, 6384−6392.
Sullivan, F. X., & Cech, T. R. (1985) *Cell 42*, 639−648.
Tanner, N. K., & Cech, T. R. (1987) *Biochemistry 26*, 3330−3340.
Walstrum, S. A., & Uhlenbeck, O. C. (1990) *Biochemistry 29*, 10573−10576.
Yarus, M., Illangesekare, M., & Christian, E. (1991) *J. Mol. Biol. 222*, 995−1012.
Zaug, A., Grosshans, C. A., & Cech, T. R. (1988) *Biochemistry 27*, 8924−8931.

BI951962Z